Journal of Ceramic Processing Research. Vol. 9, No. 6, pp. 569~575 (2008)

J O U R N A L O F
Ceramic Processing Research

Computational modeling of the sintering process of ceramic particles in a fluidized bed furnace

Chang-Il Ahn[a], Jin-Bok Yoo[a], Yoo-Taek Kim[b] and Sung-Chul Yi[a,*]
[a]*Department of Chemical Engineering, Hanyang University, Seoul 133-791, Korea*
[b]*Department of Materials Engineering, Kyonggi University, Suwon 443-760, Korea*

The sintering process of ceramic particles is a gas-solid two-phase flow, which is frequently encountered in many industrial fluid flow processes. This paper presents a computational modeling study of gas-solid flow in a fluidized bed furnace by means of three-dimensional computational fluid dynamics (CFD) and a discrete phase model (DPM) using a commercial computational fluid dynamics code, FLUENT® 6.3.26. The motion of ceramic particles is calculated by DPM. In DPM, the flow of hot air is described by a momentum conservation equation. A simulation is performed in the furnace by varying the additional inlet mass flow rates and the distributor's hole diameter across the values 2.2 mm, 1.8 mm, 1.4 mm and 1.0 mm. Through this simulation, it is possible to visually observe the temperature and velocity distribution inside the furnace, and we can optimize the process parameters such as hole diameter of the distributor and mass flow rates of an additional inlet for the sintering of the ceramic particles. Numerical results of a three-dimensional fluidized bed are compared to experimental results in order to validate this model.

Key words: Fluidized bed, Discrete Phase Model (DPM), Computational Fluid Dynamics (CFD), Gas-Particle flow.

Introduction

A gas flow including small particles in a fluidized bed is used in many chemical and material processes. Fluidized bed reactors are widely used in drying, coating, the pharmaceutical, refining and petroleum industries, and in gasification of coal because of good heat and mass transfer efficiency. This is due to strong mixing that enhances particles-fluid contact as well as improving heat and mass transfer between particles and the gas, a low temperature gradient in the reactor, and simple operation.

The sintering process of ceramic particles is performed at a very high temperature, so it is impossible to observe the internal part of the fluidized bed furnace. Therefore, to calculate the trajectories of the ceramic particles, fluid velocity and temperature distributions, numerical simulation of the gas-particle flow is done by adopting the CFD technique.

Gas-solid two-phase flow simulations can be classified into two main categories : the Eulerian–Eulerian approach and the Eulerian-Lagrangian approach. In the Eulerian-Eulerian approach (Two Fluid Model, TFM), the gas and the solid phase are considered as a fully interpenetrating continuum [1] because the small particles in the fluidized bed behave like a fluid phase due to the fluidization phenomena. Over the past few decades, a considerable number of studies have been conducted on fluidized bed modeling using the two-fluid model approach. A kinetic theory of granular particles was developed using gas-solid bubbling fluidized beds by Ding and Gidaspow (1990) [2]. Taghipour et al. (2005) [3] compared the simulation data with the experimental data in a 2D fluidized bed column. Owoyemi and Lettieri (2005) [4] also validated the numerical simulation data with the experimental results from industrial rutile powders.

Tremendous advances in computer technology have made it possible to directly calculate the particle trajectories by DPM [5]. In the Eulerian-Lagrangian approach (DPM), the motion of the solid phase is calculated by a discrete method, which applies the Newton's laws of motion to individual particles, and the flow of the gas phase is treated as a continuum. Since Cundall and Strack (1979) [6] first proposed the DPM approach, many researchers have carried out discrete phase simulations using the Eulerian-Lagrangian approach. Tsuji et al. (1993) [7] dealt with a spouting bed where gas issued from a small nozzle experimentally and numerically. Hoomans et al. (1995) [8] studied bubble and slug formation in a 2D gas-fluidized bed with uniform particles. Li and Mason (2000) [9] performed numerical modeling for a gas-solid two-phase flow with heat transfer in pneumatic transport pipes. Chiesa et al. (2005) [1] compared numerical results by both the Eulerian-Eulerian approach and the Eulerian-Lagrangian approach with experimental observations. Shah et al. (2007) [10] simulated a complete powder coating process using a commercial CFD code, FLUENT® 6.1. Fidaros et al. (2007) [11] presented all the necessary flow, heat and mass transfer and chemical reaction models considering the influence of turbulence by a two-equation (k-ε) model.

Although several studies have been carried out using a

*Corresponding author:
Tel : +82-2-2220-0481
Fax: +82-2-2298-5147
E-mail: scyi@hanyang.ac.kr

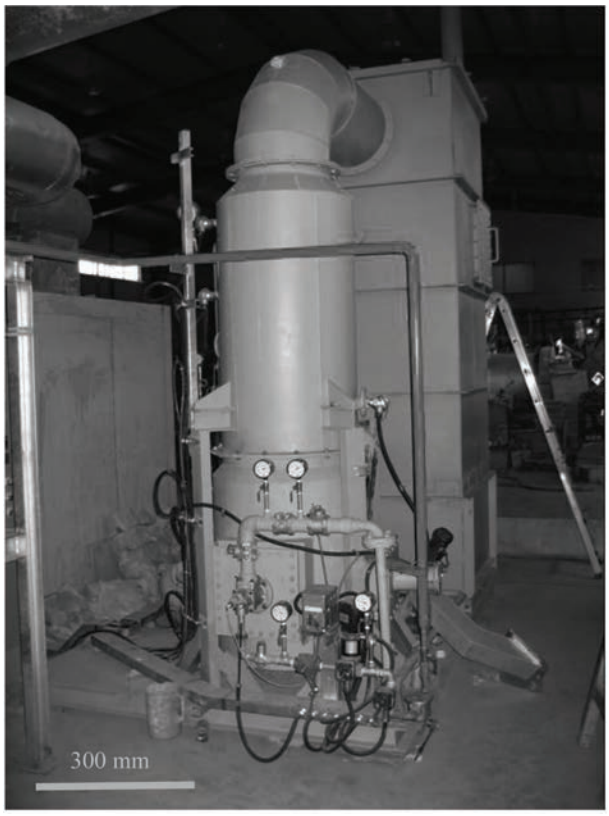

Fig. 1. Experimental apparatus of a fluidized bed furnace.

two-dimensional fluidized modeling adopting Eulerian-Eulerian approach or Eulerian-Lagranian approach, few attempts have been made on a three-dimensional fine grid modeling of the fluidized bed.

In this paper, gas-solid flow in the fluidized bed was simulated using a commercial CFD code, FLUENT® 6.3.26 with roughly 1.5 million computational cells. We have conducted the present research in order to find the optimal operating conditions of the fluidized bed for the production of porous ceramic particles.

Mathematical model

Model description

The experimental apparatus is shown schematically in Fig. 1. This apparatus is a system that sinters spherical ceramic particles at a high temperature. Fig. 2. shows a system schematic of a three-dimensional fluidized bed system. The simplified system consists of two air inlets, one raw material inlet, one outlet, a distributor and a furnace. Hot air is injected into the furnace and is spouted out vertically onto the distributor plates. When the gas velocity reaches a critical value at which the upward drag forces equal gravity, the ceramic particles are suspended within the hot air. Heat transfers from hot air to ceramic particles.

Model assumptions

The proposed model includes several assumptions:

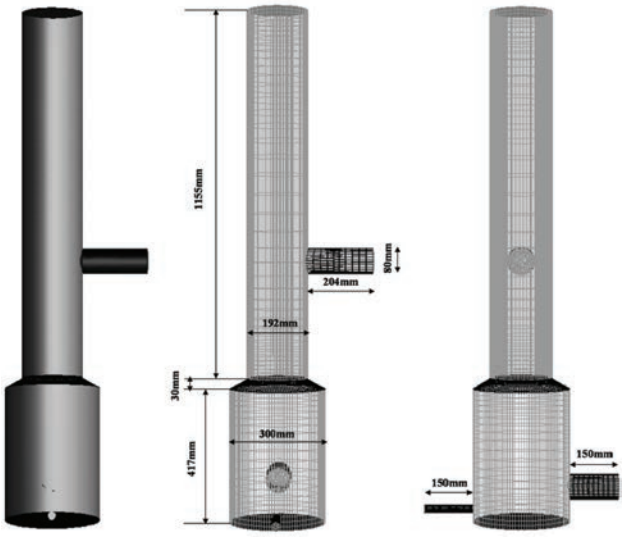

Fig. 2. Schematic diagram of a simplified fluidized bed furnace.

(i) The flow is three-dimensional and steady.
(ii) The flow is air, incompressible and turbulent.
(iii) The inner wall of the furnace is adiabatic.
(iv) Radiative heat transfer is neglected.
(v) Particle diameters are uniform.
(vi) Particles are ideal spheres.

Governing equations

The gas-phase

A three-dimensional, incompressible, steady mathematical model was developed to describe gas-solid multiphase flow in the fluidized bed.

The conservation of mass was described by a continuity equation:

$$\nabla\cdot(\rho u)=0 \tag{1}$$

The calculation of the gas motion was performed using a generalized form of a momentum conservation equation:

$$\nabla\cdot(\rho uu)=-\nabla p+\nabla\cdot(\tau)+\rho g+F \text{-} \tag{2}$$

$$\text{where } \tau=\mu\left[(\nabla u+\nabla u^{T})-\frac{2}{3}\nabla\cdot uI\right] \tag{3}$$

The gas flow was considered to be a weak turbulent flow. So we have made use of a standard k-ε model [9]. Transport equations for the standard k-ε turbulence model can be written as:

$$\frac{\partial}{\partial x_i}(\rho k u_i)=\frac{\partial}{\partial x_j}\left[\left(\mu+\frac{\mu_t}{\sigma_k}\right)\frac{\partial k}{\partial x_j}\right]+G_k+G_b-\rho\varepsilon-Y_M \tag{4}$$

and

$$\frac{\partial}{\partial x_i}(\rho\varepsilon u_i)=\frac{\partial}{\partial x_j}\left[\left(\mu+\frac{\mu_t}{\sigma_\varepsilon}\right)\frac{\partial\varepsilon}{\partial x_j}\right]$$
$$+C_{1\varepsilon}\frac{\varepsilon}{k}(G_k+C_{3\varepsilon}G_b)-C_{2\varepsilon}\rho\frac{\varepsilon^2}{k} \tag{5}$$

Conservation of energy is expressed as:

$$\nabla\cdot(u(\rho E+p))=\nabla\cdot(k_{eff}\nabla T-\sum_j h_j J_j+(\tau_{eff}\cdot u))+S_h \quad (6)$$

The discrete solid-phase

Particle-particle interactions were neglected due to the low volumetric fraction of solid phase (below 10%). Particle motion in a flow field was calculated using Newton's second law of motion :

$$\frac{du_p}{dt}=F_D(u-u_p)+\frac{g(\rho_p-\rho)}{\rho_p}+F_i \quad (7)$$

where $F_D(u-u_p)$ is the drag force per unit particle mass and:

$$F_D=\frac{18\mu}{\rho_p d_p^2}\frac{C_D Re_p}{24} \quad (8)$$

The particle Reynolds number is:

$$Re_p=\frac{\rho d_p|u_p-u|}{\mu} \quad (9)$$

The drag coefficient C_D is expressed as a function of the particle Reynolds number:

$$C_d=\frac{24}{Re_p}(1+b_1 Re_p^{b_2})+\frac{b_3 Re_p}{b_4+Re_p} \quad (10)$$

where [12]

$b_1=\exp(2.3288-6.4581\phi+2.4486\phi^2$

$b_2=0.0964+0.5565\phi$

$b_3=\exp(4.905-13.8944\phi+18.4222\phi^2-10.2599\phi^3$

$b_4=\exp(1.4681+12.2584\phi-20.7322\phi^2+15.8855^3 \quad (11)$

we assumed that the ceramic particles were perfectly spherical, so ϕ is considered as 1.

Numerical procedures

Although the Semi-Implicit Method for Pressure-Linked Equation (SIMPLE) [13] is often used for calculating governing equations in two-dimensional fluidized bed system, the SIMPLEC (SIMPLE Consistent) algorithm is used for fine grid systems due to its short computational time. The SIMPLEC algorithm is recommended for the solution of incompressible fluid flow and heat transfer problems, especially when the grid density is fine [14]. Computations were performed adopting the SIMPLEC algorithm in this paper.

In this research, mathematical modeling of the three-dimensional fluidized bed was implemented with a commercially available computational fluid dynamics code, FLUENT. Approximately 1,500,000 computational cells were used in all the simulations.

Results and Discussion

Experiment

A three-dimensional experimental fluidized bed furnace, which is used for production of porous ceramic particles is shown in Fig. 1 The hole diameter of a distributor in the experimental apparatus is 2.2 mm. The bed was shallowly fluidized by compressed hot air onto the distributor. Injected ceramic particles were spouted onto the distributor, moved upwards to a height of about 5-8 cm, were suspended in the air and fell down on the distributor due to the gravitational force. Experimental results [15] are shown in Fig. 3. As the range of suspension increased and broadened, more particles stayed longer in the fluidized bed. Fluid-to-particle heat transfer in a vertical moving bed of solids with air flow was activated. Therefore, parametric

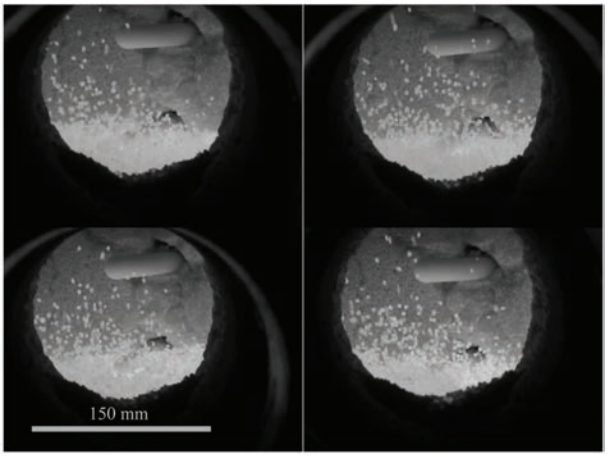

Fig. 3. Experimental results of particle motion (hole diameter, 2.2 mm).

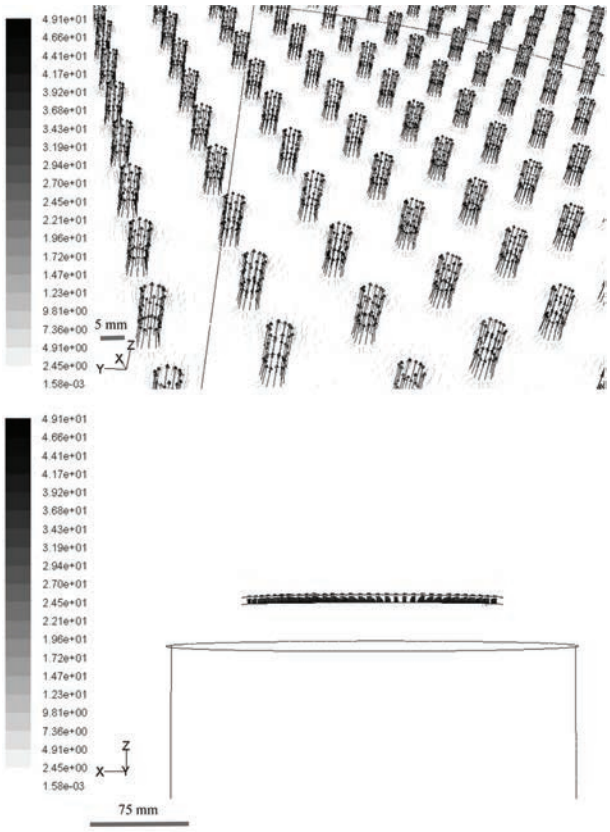

Fig. 4. Velocity profiles onto the distributor (hole diameter, 2.2 mm).

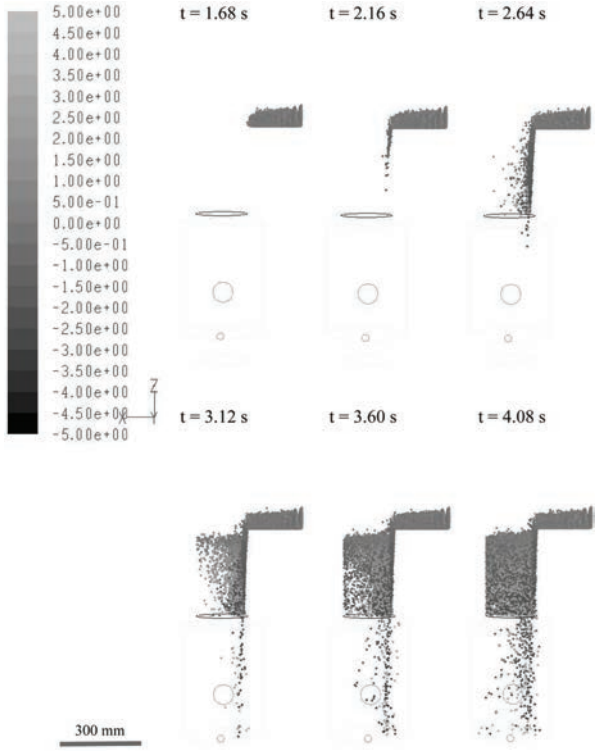

Fig. 5. Behavior of particles in the furnace (hole diameter, 2.2 mm).

studies for an increase in the suspension range are necessary.

Numerically calculated results are shown in Figs. 4 and 5 Input parameters used in the model and boundary conditions are listed in Table 1 and Table 2. Spouting velocity was 49.1 m/s onto the distributor. The motion of particles can be observed in Fig. 5. by many points. Results were slightly different from the experiments, but the overall tendency of the motion of particles was similar to the experimental results. We guessed that a cause of the difference between the experimental results and numerical data probably arouse from a density change of particles due to agglomeration of raw materials.

Table 1. Boundary conditions

First air flow inlet (kg/s)	0.00694444
Second air flow inlet (kg/s)	0.000186 to 0.00093
Particle inlet (kg/s)	0.00333
Outlet pressure (Pa)	0 (Gauge pressure)

Table 2. Input parameters used in the modeling

Particles	
Shape	spherical
Diamter (mm)	1.8
Density (kg/m^3)	1500
Gas	
Density (kg/m^3)	0.243
Viscosity (kg/m·s)	5.444e-5
Thermal conductivity(W/m·K)	0.0242
Specific heat capacity(J/kg·K)	1006.43

The effect of the hole diameter of a distributor

To obtain the optimal condition for fluidization, parametric studies were performed at various hole diameters of the

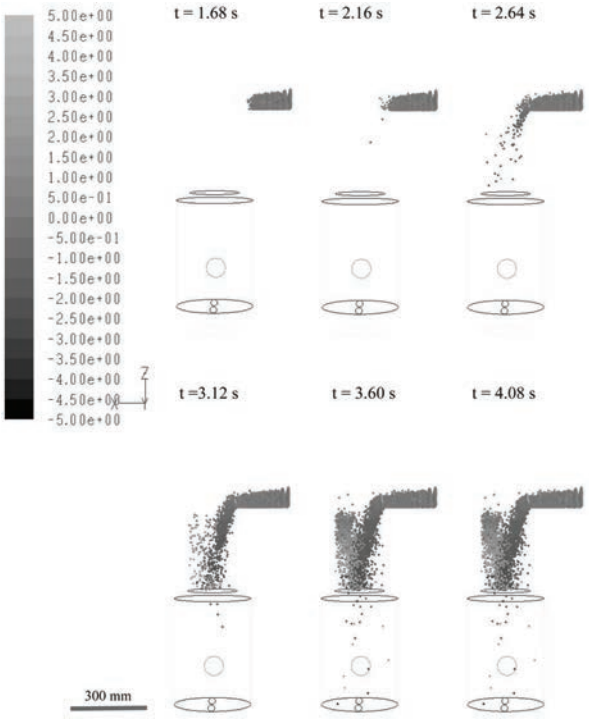

Fig. 6. Behavior of particles in the furnace (hole diameter, 1.8 mm).

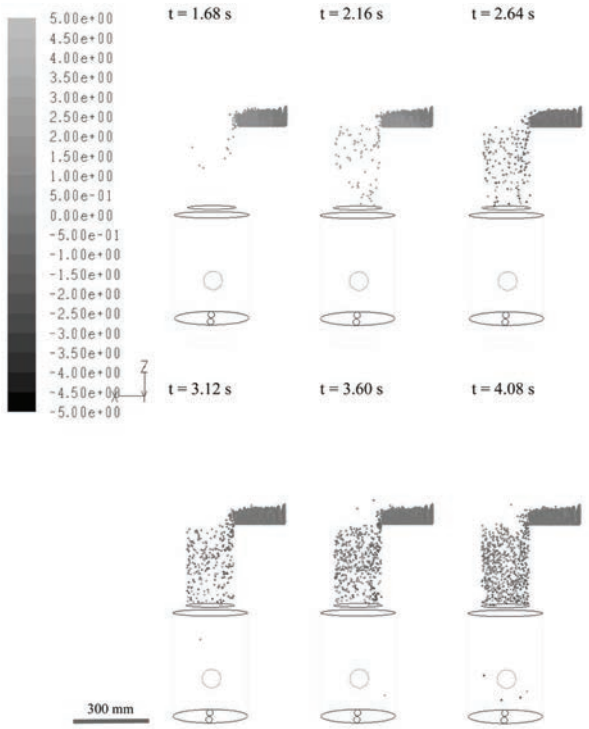

Fig. 7. Behavior of particles in the furnace (hole diameter, 1.4 mm).

distributor. The hole diameters varied from 2.2 mm to 1.0 mm.

Fig. 6 shows the numerical results of particle motions with a 1.8 mm hole diameter of the distributor. The suspension height of ceramic particles gradually increased in comparison with the case of the hole diameter 2.2 mm and the number of particles moving in the downward direction was somewhat diminished.

The trajectories of ceramic particles with a 1.4 mm hole diameter of distributor are shown in Fig. 7. The suspension height of particles was approximately 29.8 cm and the maximum height did not exceed 32.5 cm. The particle brightness indicate particle's z-direction velocity. As the diagram indicates, we can see that particle velocity gradually slowed, became zero, and fell down on the distributor. Suspension height of particles became slightly higher compared to the cases of 2.2 mm, 1.8 mm. In comparison with the numerical results of hole diameter 2.2 mm, more particles had a positive z-velocity in the results of 1.8 mm, 1.4 mm. We confirmed that the suspension height in particle motions got higher in Fig. 8 in comparison with the results of Figs. 5-7.

Fig. 9 shows a temperature profile and temperature variation above the distributor. We could confirm that temperature was diminished due to fluid-to-particle heat transfer.

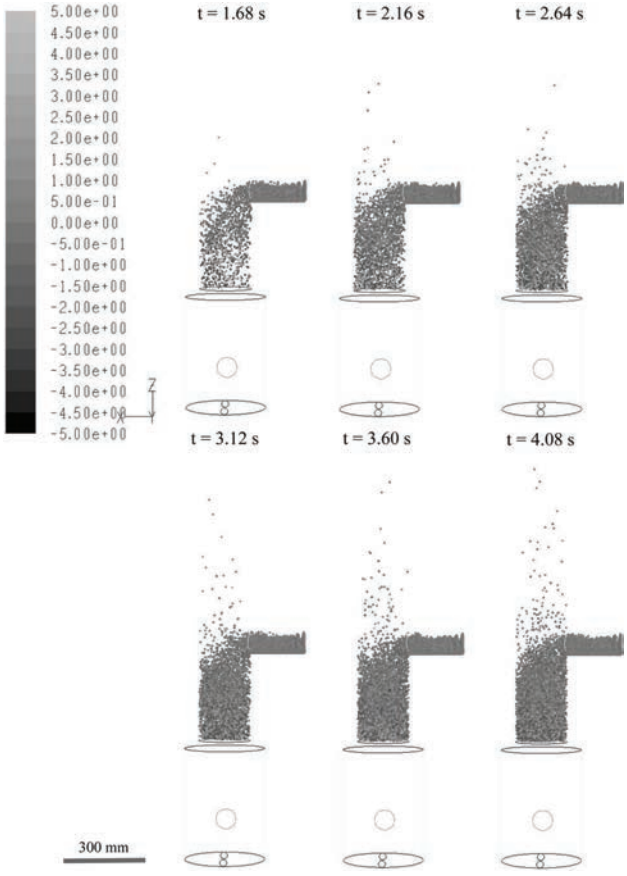

Fig. 8. Behavior of particles in the furnace (hole diameter, 1.0 mm, 0.000186 kg/s)

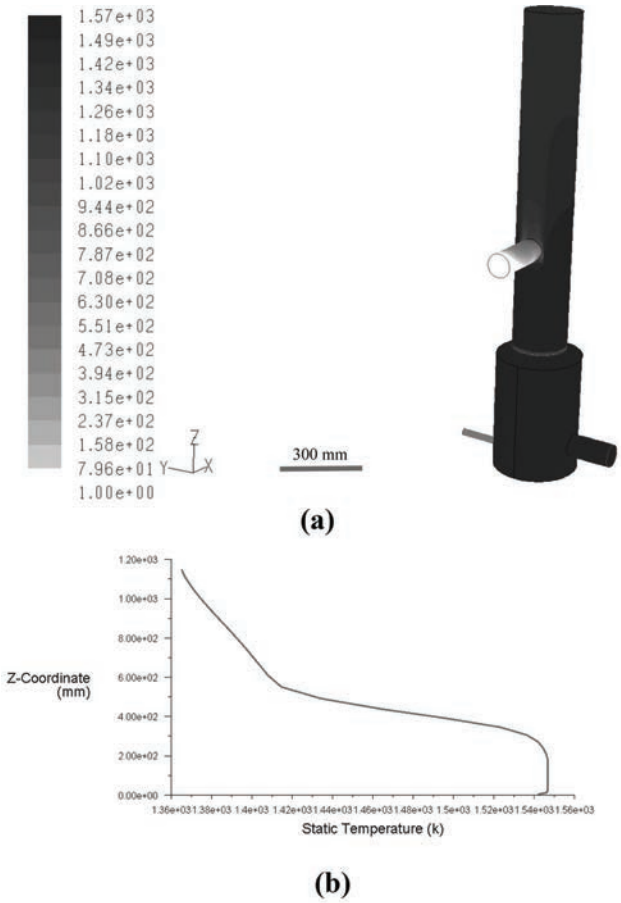

Fig. 9. Temperature distribution in the fluidized bed furnace.

Fig. 10 shows z-velocity distributions at various hole diameters of the distributor. Distributions of particle z-velocity were suddenly wider after 1.5 seconds. The sudden expansion of width was likely to have been caused by the movement of particles from the raw material inlet to the fluidized bed. We guess that particles started to vibrate upward and downward due to strongly spouted air at 1.5 seconds. At 1.0 mm, a calculated particle velocity above 4.0 m/s was observed.

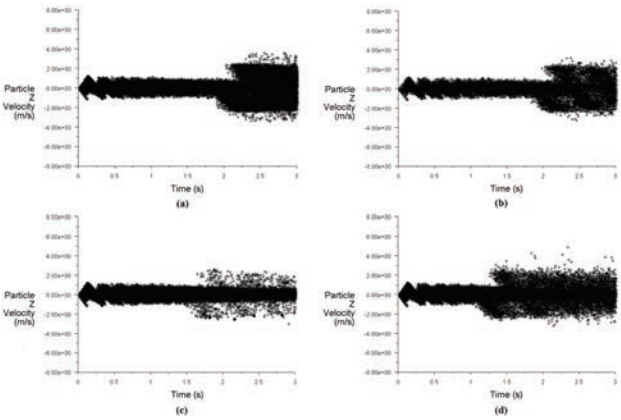

Fig. 10. Particle z-velocity distribution at various hole diameter of the distributor (a) 2.2 mm (b) 1.8 mm (c) 1.4 mm (d) 1.0 mm.

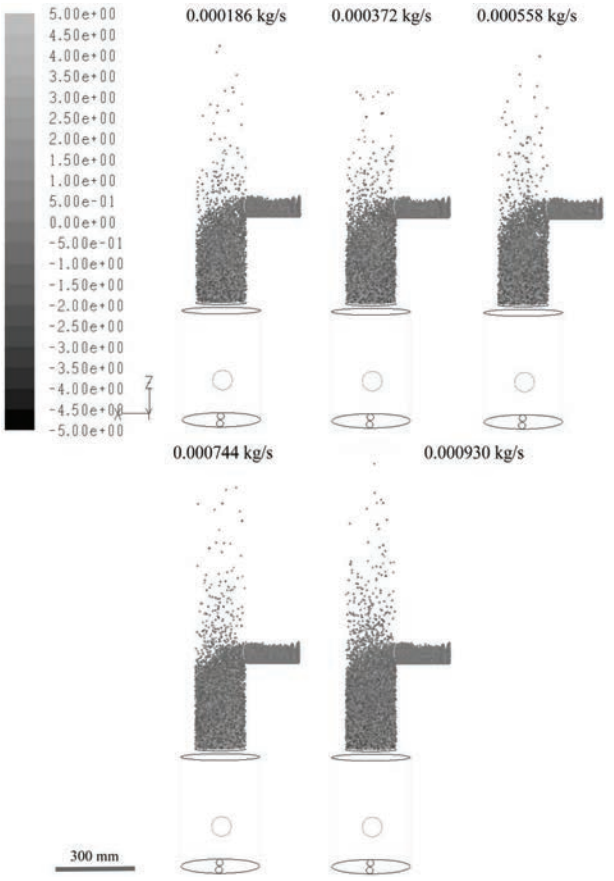

Fig. 11. Behavior of particles at various additional mass flow rate inlet (hole diameter, 1.0 mm, t = 4.08 s)

The effect of the mass flow inlet of air

The dependency of particle motion on parameters such as mass flow rates of an additional inlet was investigated. With the distributor, an additional flow inlet is also necessary to give a higher pressure gradient which causes fluidization between the inlet and outlet sides of holes of the distributor.

Fig. 8 and Fig. 11 showed snapshots of particle configurations at various additional mass inlet flow rates. We were able to confirm there was no great difference in particle motion from 0.000186 kg/s to 0.000930 kg/s.

Conclusions

A three-dimensional mathematical modeling for a fluidized bed furnace was carried out for the prediction of velocity, temperature and particle motion. We assumed that the flow system had already become steady-state and the calculation of particle trajectories were performed under unsteady-state conditions. To obtain an optimal condition for sintering and fluidization, parametric studies were conducted.

In this research, suspension height of particles gradually increased with a decrease of hole diameter, conspicuously increased at about 1.0 mm. The simulations were found to depend strongly on the value of the hole diameter of the distributor.

Consequently, we can conclude that an optimal value of the hole diameter of the distributor was around 1.0 mm. In comparison with the effect of the hole diameter of the distributor on particle motion, the effect of the mass flow rate of an additional inlet on particle motion was insignificant.

The pressure gradient below 1.0 mm in hole diameter may increase as compared to the results of 1.0 mm-2.2 mm but particles affected by upward airflow may be diminished due to the decrease of the surface area of the hole outlet. Because an excessive pressurization by a shrinking hole causes additional wear and tear on ceramic particles, we did not consider a hole diameter below 1.0 mm.

Acknowledgements

This research is supported by the Resource Recycling R&D center, 21C Frontier R&D program and authors gratefully appreciate it.

Nomenclature

List of symbols

C_D : the drag coefficient
D : particle diameter [mm]
E : total energy [J/kg]
$\mathbf{F}$: the external body force [N/m^3]
F_D : coefficient for drag force [1/s]
$\mathbf{F}_i$: the additional acceleration [N/kg]
$\mathbf{G}$: gravitational acceleration [m/s^2]
G_b : the generation of turbulence kinetic energy due to buoyancy [J/m^3·s]
G_k : the generation of turbulence kinetic energy due to the mean velocity gradients [J/m^3·s]
h_j : species enthalpy [J/kg]
$\mathbf{I}$: the unit tensor [Pa]
$\mathbf{J}_j$: diffusion flux [kg/m^2·s]
k : kinetic energy per unit mass [J/kg]
k_{eff} : the effective conductivity [W/m·K]
P : pressure [Pa]
Re_p : the particle Reynolds number
S_h : volumetric heat source [J/m^3 · s]
$\mathbf{u}$: overall velocity vector [m/s]
$\mathbf{u}_p$: the particle velocity [m/s]

Greek

ε : Turbulent dissipation rate [m^2/s^3]
μ : the molecular viscosity of the fluid [kg/m · s]
ρ : density [kg/m^3]
ϕ : the shape factor
τ : stress tensor [Pa]

References

1. M. Chiesa, V. Mathiesen, J.A. Melheim and B. Halvorsen, Computers and Chemical Engineering 29 (2005) 291-304.
2. L. Huilin, Z. Yunhua, J. Ding, D. Gidaspow and L. Wei, Chemical Engineering Science 62 (2007) 301-317.
3. F. Taghipour, N. Ellis and C. Wong, Chemical Engineering Science 60 (2005) 6857-6867.
4. O. Owoyemi and P. Lettieri, Industrial Engineering Chemistry Research 44 (2005) 9996-10004.
5. J. Ouyang and J. Li, Chemical Engineering Science 54 (1999) 5427-5440.
6. P.A. Cundall and O.D.L. Strack, Gotechnique 29 (1979) 47.
7. Y. Tsuji, T. Kawaguchi and T. Tanaka, Powder Technology 77 (1993) 79-87.
8. B.P.B. Hoomans, J.A.M. Kuipers, W.J. Briels and W.P.M. Van Swaaij, Chemical Engineering Science 51 (1996) 99-118.
9. J. Li and D.J. Mason, Powder Technology 112 (2000) 273-282.
10. U. Shah, C. Zhang, J. Zhu, F. Wang and R. Martinuzzi, International Journal of Multiphase Flow 33 (2007) 557-573.
11. D.K. Fidaros, C.A. Baxevanou, C.D. Dritselis and N.S. Vlachos, Powder Technology 171 (2007) 81-95.
12. A. Haider and O. Levenspiel, Powder Technology 58 (1989) 63-70.
13. Suhas V. Patankar, Numerical Heat Transfer and Fluid Flow, Hemisphere Publishing Corporation (1980).
14. M. Zeng and W.Q. Tao, Engineering Computations 20 (2003) 320-340.
15. K. Kim, Y. Kim, S. Kang, K-G. Lee and J-H. Kim, International Symposium of Resource Recycling (2007).